

## Short communication

Preparation of  $\text{Li}_{1.5}\text{Al}_{0.5}\text{Ti}_{1.5}(\text{PO}_4)_3$  solid electrolyte via a sol–gel route using various Al sources

Masashi Kotobuki\*, Masaki Koishi

Department of Material and Environmental Engineering, Hakodate National College of Technology, 14-1 Tokura-cho, Hakodate, Hokkaido 042-8501, Japan

Received 10 August 2012; received in revised form 13 October 2012; accepted 13 October 2012

Available online 22 October 2012

## Abstract

$\text{Li}_{1.5}\text{Al}_{0.5}\text{Ti}_{1.5}(\text{PO}_4)_3$  (LATP) has received much attention as a solid electrolyte for lithium ion batteries due to its high Li ion conductivity. In this study, the LATP is prepared by a sol–gel process using water-soluble  $\text{Al}(\text{NO}_3)_3$  and water-insoluble  $\text{Al}(\text{C}_3\text{H}_7\text{O})_3$  as Al sources to examine the influence of the Al source on the properties of the produced LATP. The LATP is successfully produced in both cases; however, a small amount of  $\text{AlPO}_4$  impurity is formed in the  $\text{Al}(\text{NO}_3)_3$  sample due to insufficient mixing of the water-insoluble  $\text{Ti}(\text{C}_3\text{H}_7\text{O})_4$  with the water-soluble  $\text{Al}(\text{NO}_3)_3$ . In contrast, the  $\text{AlPO}_4$  formation is not observed in the  $\text{Al}(\text{C}_3\text{H}_7\text{O})_3$  sample. The Li ion conductivity of the  $\text{Al}(\text{C}_3\text{H}_7\text{O})_3$  sample is higher than that of the  $\text{Al}(\text{NO}_3)_3$  sample, implying that the  $\text{AlPO}_4$  impurity acts as a resistance layer. The performance of LATP prepared by the sol–gel method is strongly affected by the Al sources, and the water-insoluble Al source is suitable for water-insoluble  $\text{Ti}(\text{C}_3\text{H}_7\text{O})_4$ , which has been the most widely used Ti source to date.

© 2012 Elsevier Ltd and Techna Group S.r.l. All rights reserved.

Keywords: Solid electrolyte; Lithium battery; Sol–gel method

## 1. Introduction

Rechargeable batteries have played a key role in our present information-rich world [1]. Many types of rechargeable batteries have been developed thus far. Among them, the rechargeable Li ion battery has been recognized as the most suitable battery for mobile information devices due to its high energy and power densities.

A source of the high powder density of the Li ion battery is its high operation voltage as the power density is the product of the operation voltage by the electric current density. However, under the high operation voltages of Li ion batteries ( $\sim 3.8$  V), water, which is used as an electrolyte in most batteries, is decomposed into hydrogen and oxygen. Thus, flammable organic electrolytes, which can tolerate such high voltages, must be used instead, to avoid inherent safety issues, such as explosion.

To solve this safety problem, inflammable ceramic electrolytes have been studied [2–10]. Batteries with ceramic

electrolytes, called all-solid-state batteries, can completely eliminate the flammable components in the battery and has been considered the ultimate safe battery. The  $\text{Li}_{1.5}\text{Al}_{0.5}\text{Ti}_{1.5}(\text{PO}_4)_3$  (LATP) solid electrolyte is a Li-ion-conductive ceramic with Na super ion conductor (NASICON) structure. Its Li ion conductivity was reported as  $\sim 10^{-3} \text{ S cm}^{-1}$  [11], which is very close to that of the organic electrolyte currently used in the rechargeable Li ion battery. Therefore, LATP has received much attention for its all-solid-state battery applications [12].

The LATP has been prepared using melt-quenching and solid solution methods [13,14]. However, these methods require high-temperature processing at over  $1200^\circ\text{C}$ . To conserve energy, a low-temperature preparation process has been strongly called for. A sol–gel method allows us to prepare inorganic materials at low temperatures [15]. Some groups have succeeded in preparing LATP by the sol–gel method. However, systematic research with respect to the preparation of LATP using sol–gel processes has not yet been reported. For example, Takada et al. used  $\text{LiOC}_2\text{H}_5$ ,  $\text{Ti}(\text{OC}_3\text{H}_7)_4$ , and  $\text{PO}(\text{OC}_2\text{H}_5)_{3-x}$  to prepare LATP [16]. However, Xu et al. reported the electrochemical properties

\*Corresponding author. Tel./fax: +81 138 59 6466.

E-mail address: [kotobuki@hakodate-ct.ac.jp](mailto:kotobuki@hakodate-ct.ac.jp) (M. Kotobuki).

of LATP prepared from  $\text{Ti}(\text{OC}_4\text{H}_9)_4$ ,  $\text{LiNO}_3$ ,  $\text{Al}(\text{NO}_3)_3$ , and  $\text{NH}_4\text{H}_2\text{PO}_4$  [17]. All of these previous studies have been performed using different starting materials and preparation conditions. Therefore, a study on the influence of the starting material for LATP preparation on the nature of the final product would be quite helpful.

In this paper, the effect of Al source on the properties of the LATP solid electrolyte prepared by the sol–gel method was studied. Water-soluble  $\text{Al}(\text{NO}_3)_3$  and water-insoluble  $\text{Al}(\text{C}_3\text{H}_7\text{O})_3$  were used as Al sources for LATP preparation, and the final products were characterized.

## 2. Experimental

The LATP solid electrolyte was prepared by the sol–gel method [12,18]. A precursor sol for LATP was prepared by mixing  $\text{CH}_3\text{COOLi}$ ,  $\text{Al}(\text{C}_3\text{H}_7\text{O})_3$ ,  $\text{Ti}(\text{C}_3\text{H}_7\text{O})_4$ ,  $\text{H}_3\text{PO}_4$ , iso-

propanol,  $\text{CH}_3\text{COOH}$ , and  $\text{H}_2\text{O}$  in a molar ratio of 3:1:3:6:100:50:700. In another batch, water-soluble  $\text{Al}(\text{NO}_3)_3$  was used instead of water-insoluble  $\text{Al}(\text{C}_3\text{H}_7\text{O})_3$  to investigate the influence of Al source on the final product. All reagents were purchased from Wako Chemical Co. Ltd, Japan and used without further purification. The precursor sol was dried at 100 °C for gelation, and the obtained gel was heated at 450 °C for 4 h in air. The powder was milled by a planetary ball mill (Pulver Risetete 7, Fritsch) at 400 rpm for 1 h and then pressed into pellet form with 20 mm diameter. The pellet was calcined at 1000 °C for 6 h.

The crystalline phases of the heated powder and calcined pellet were identified with X-ray diffraction (XRD, Rigaku Ultima-IV) using  $\text{Cu-K}\alpha$  radiation. Scanning electron microscopy (SEM, JEOL, JSM-6300LA) was used to observe the morphology of the powder and the pellet cross-section.

The Li ion conductivity was measured by the AC impedance method. Prior to measurement, Au was sputtered onto both sides of the pellet to ensure electrical contact. The AC impedance data were collected at  $\pm 5$  mV voltage signal in a frequency range of 4–1 MHz using a chemical impedance meter (HIOKI Chemical Impedance Meter 3532-80). The measurement was performed at 30–200 °C to clarify the temperature dependency of Li ion conductivity.

## 3. Results

### 3.1. Characterization of LATP prepared by the sol–gel method using various Al sources

Fig. 1 showed the XRD patterns of powder prepared by the sol–gel method after heating at 450 °C for 4 h. No clear

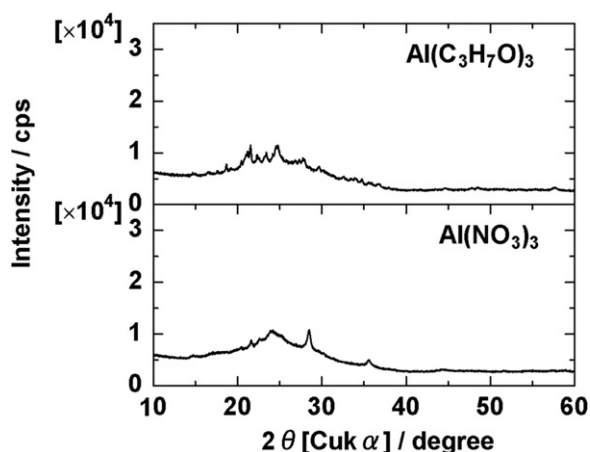


Fig. 1. XRD patterns of powders prepared by the sol–gel method using various Al sources after heating at 450 °C for 4 h.

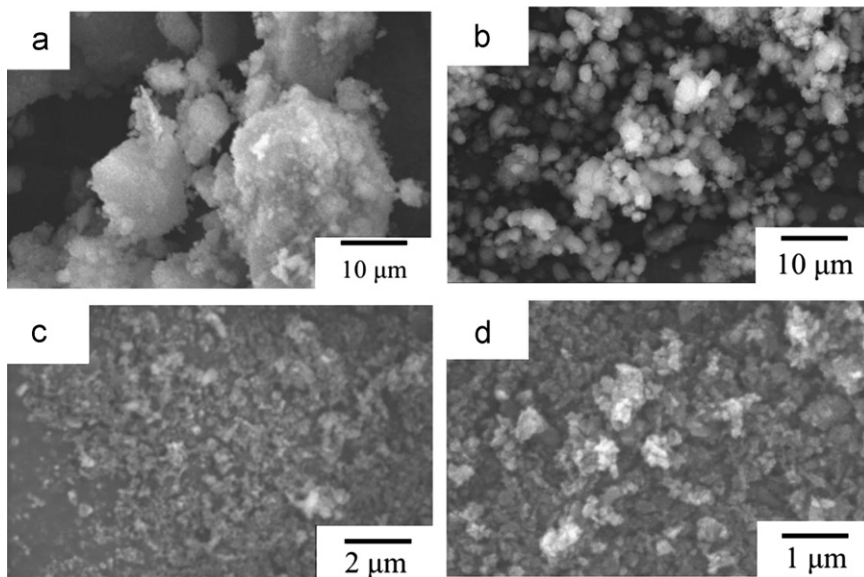


Fig. 2. SEM images of powders prepared by the sol–gel method using various Al sources after heating at 450 °C for 4 h before and after ball-milling. (a)  $\text{Al}(\text{C}_3\text{H}_7\text{O})_3$ , (b)  $\text{Al}(\text{NO}_3)_3$ , (c)  $\text{Al}(\text{C}_3\text{H}_7\text{O})_3$  after ball-milling and (d)  $\text{Al}(\text{NO}_3)_3$  after ball-milling.

diffraction peak was observed in all patterns, implying that the powder after calcination at 450 °C was primarily amorphous. In the  $\text{Al}(\text{C}_3\text{H}_7\text{O})_3$  sample, small diffraction peaks appeared at  $2\theta=20\text{--}30^\circ$ ; these peaks were not observed in the  $\text{Al}(\text{NO}_3)_3$  sample, but a peak was found at  $2\theta=28.5^\circ$ . SEM images of the powder prepared from  $\text{Al}(\text{C}_3\text{H}_7\text{O})_3$  and  $\text{Al}(\text{NO}_3)_3$  are displayed in Fig. 2a and b, respectively. Notably, both powders have completely different morphologies. The powder prepared from  $\text{Al}(\text{NO}_3)_3$  was spherical with a particle size of approximately 1–2  $\mu\text{m}$ , whereas the particle size was much larger and the shape was irregular in the  $\text{Al}(\text{C}_3\text{H}_7\text{O})_3$  sample. Both powders were milled by the planetary ball mill equipment (Fig. 2c and d) and crushed to a diameter of  $\sim 100\text{ nm}$ . The morphology difference confirmed before the milling was not observed.

The milled powder was supplied to form the pellet, which was then calcined at 1000 °C for 6 h. The XRD patterns of the calcined pellet were depicted in Fig. 3. In  $\text{Al}(\text{C}_3\text{H}_7\text{O})_3$  (Fig. 3a), all diffraction peaks are attributed to  $\text{LiTi}_2(\text{PO}_4)_3$  (PDF 35-0754) with a NASICON-type structure, indicating that the LATP solid electrolyte was successfully prepared by our sol–gel process. In the case of  $\text{Al}(\text{NO}_3)_3$ , a small peak originating from  $\text{AlPO}_4$  (PDF 00-0114) was observed in the main peaks of the LATP. Cross-sectional SEM images of the LATP pellet prepared by the sol–gel method using different Al sources are presented in Fig. 4. The pellets were sintered well, regardless of Al source at a calcination temperature of 1000 °C. Many

crystal grains were observed, and the grains were in good contact with each other. No morphology differences were found in the cross-sections.

### 3.2. Electrochemical property of the LATP prepared from different Al sources through the sol–gel process

Complex impedance plots of LATP pellets using Au blocking electrodes are depicted in Fig. 5. A semicircle and a tail were observed in both samples in the high- and low-frequency ranges, respectively. This characteristic profile of the impedance plot appears often in ceramics with ion-conductive nature [19,20]. The tail can be attributed to Warburg-type impedance, which originates from the diffusion of Li ions in the blocking electrode. The intercepts of the semicircle at the high- and low-frequency sides were ascribed to inner crystal and total (inner crystal and grain boundary) impedances, respectively [22]. The bulk (inner crystal) and total Li ion conductivities of  $\text{Al}(\text{C}_3\text{H}_7\text{O})_3$  sample were estimated to  $3.1 \times 10^{-3}$  and  $4.5 \times 10^{-4}\text{ S cm}^{-1}$ , respectively. These values are comparable to previously reported values [22,23]. In contrast, the bulk and total conductivities of  $\text{Al}(\text{NO}_3)_3$  sample were  $1.2 \times 10^{-3}$  and  $7.1 \times 10^{-5}\text{ S cm}^{-1}$ , respectively. The AC impedance measurement was performed under various temperatures to depict the Arrhenius plot (Fig. 6). In both samples, the semicircle became smaller with increasing temperature and finally disappeared, implying that the bulk conductivity increased with temperature. Therefore, the bulk conductivity could not be estimated above 100 °C and 170 °C in the  $\text{Al}(\text{C}_3\text{H}_7\text{O})_3$  and  $\text{Al}(\text{NO}_3)_3$  samples, respectively. The plot was well fit by the Arrhenius equation, and the fitting accuracies ( $R^2$  factor) in all plots were greater than 0.99. The bulk and total activation energies were 0.13 and 0.28 eV, respectively, in the  $\text{Al}(\text{C}_3\text{H}_7\text{O})_3$  samples and were 0.19 and 0.35 eV in the  $\text{Al}(\text{NO}_3)_3$  samples, respectively.

## 4. Discussion

This study was performed to clarify the influence of the Al source on properties of LATP prepared by a sol–gel method. Water-soluble  $\text{Al}(\text{NO}_3)_3$  and water-insoluble  $\text{Al}(\text{C}_3\text{H}_7\text{O})_3$  were chosen as Al sources, and the properties of the resulting LATP samples were compared.

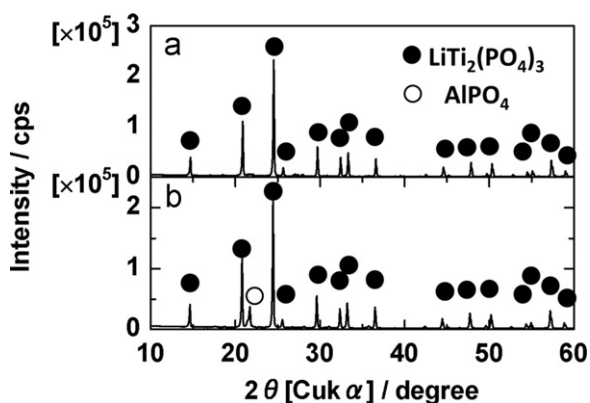


Fig. 3. XRD patterns of sintered LATP pellets prepared by the sol–gel method using (a)  $\text{Al}(\text{C}_3\text{H}_7\text{O})_3$  and (b)  $\text{Al}(\text{NO}_3)_3$  as Al sources.

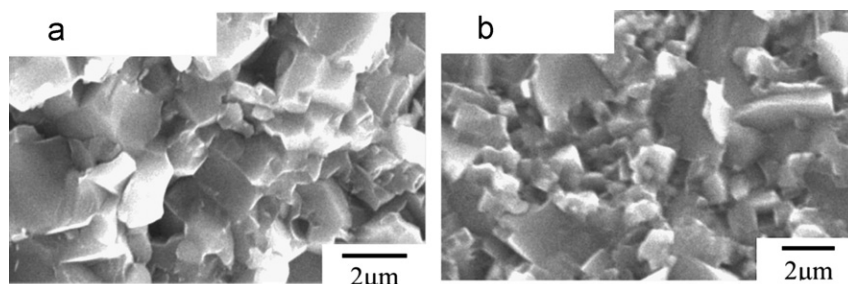


Fig. 4. Cross-sectional SEM images of sintered LATP pellets prepared by the sol–gel method using (a)  $\text{Al}(\text{C}_3\text{H}_7\text{O})_3$  and (b)  $\text{Al}(\text{NO}_3)_3$  as Al sources.

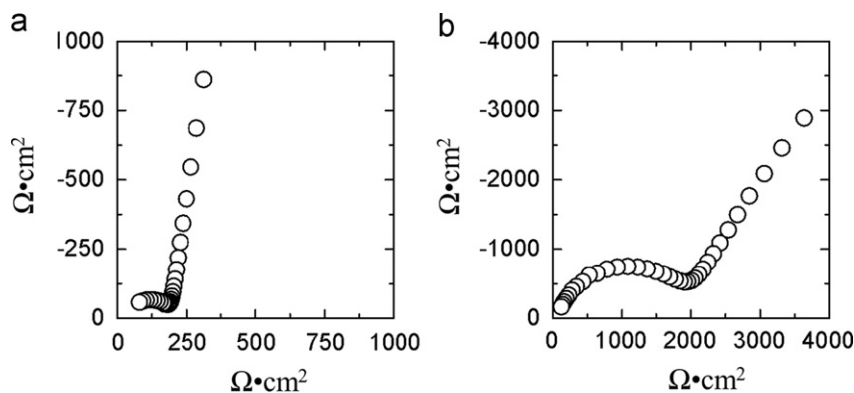


Fig. 5. Complex impedance plots of the LATP pellet prepared by the sol–gel method using (a)  $\text{Al}(\text{C}_3\text{H}_7\text{O})_3$  and (b)  $\text{Al}(\text{NO}_3)_3$  as Al sources.

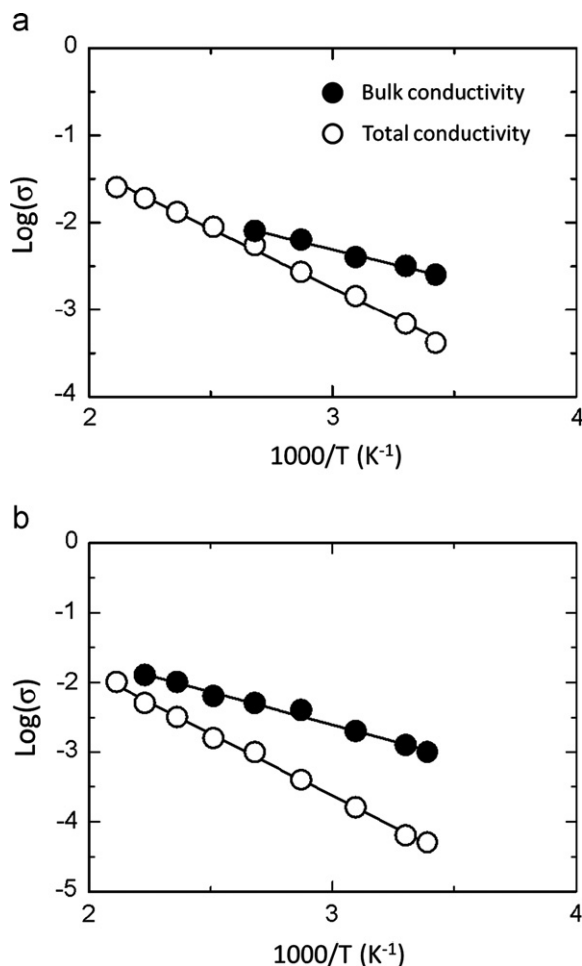


Fig. 6. Arrhenius plots of sintered pellets from (a)  $\text{Al}(\text{C}_3\text{H}_7\text{O})_3$  and (b)  $\text{Al}(\text{NO}_3)_3$ .

The XRD pattern of the sintered pellet clearly indicated that the pellet from  $\text{Al}(\text{NO}_3)_3$  contained  $\text{AlPO}_4$  with LATP, whereas all diffraction peaks could be attributed to LATP in the pellet prepared from  $\text{Al}(\text{C}_3\text{H}_7\text{O})_3$ . This difference is ascribed to the solubility of the Al source. Water-insoluble  $\text{Ti}(\text{C}_3\text{H}_7\text{O})_4$  was used as a Ti source in this study. Accordingly, the Ti source was resolved into the alcohol phase (iso-propanol in this study). Similarly, the

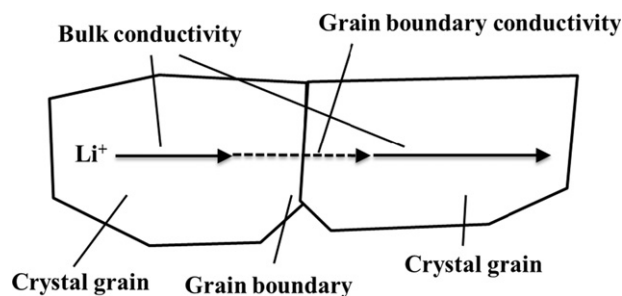


Fig. 7. Schematic illustration of Li ion conduction in ceramics.

water-insoluble  $\text{Al}(\text{C}_3\text{H}_7\text{O})_3$  was also resolved into the alcohol phase. The Ti and Al sources mixed well in the alcohol phase. In contrast, the water-soluble  $\text{Al}(\text{NO}_3)_3$  was resolved into the water phase; thus, Al in water and Ti in alcohol mixed poorly. Therefore,  $\text{AlPO}_4$  may have been formed due to insufficient mixing of Ti with the Al source. In the case of  $\text{Al}(\text{C}_3\text{H}_7\text{O})_3$ , both Al and Ti sources were in the alcohol phase and mixed well, suppressing any  $\text{AlPO}_4$  formation, which is the Ti-lacking phase of LATP.

The Li ion conductivity of the pellet prepared by  $\text{Al}(\text{C}_3\text{H}_7\text{O})_3$  was considerably higher than that prepared by  $\text{Al}(\text{NO}_3)_3$ . This behavior is thought to be due to  $\text{AlPO}_4$  formation.  $\text{AlPO}_4$  does not have a Li ion conductive nature; thus,  $\text{AlPO}_4$  would act as a resistance layer in the LATP solid electrolyte. Comparing the conductivities of both pellets, the bulk conductivities were of same order, although a large difference was confirmed in the total conductivities among them ( $4.5 \times 10^{-4}$  and  $7.1 \times 10^{-5} \text{ S cm}^{-1}$  for  $\text{Al}(\text{C}_3\text{H}_7\text{O})_3$  and  $\text{Al}(\text{NO}_3)_3$  samples, respectively). The total conductivity consists of two components, the bulk and grain boundary conductivities (Fig. 7) [21]. When the bulk conductivity is high and the grain boundary conductivity is low, the Li ion can migrate very fast in the bulk, but very slow at grain boundary. In this case, the total conductivity is lower than the bulk one, because the grain boundary conductivity dominates the total conductivity. Therefore, the large difference in the total conductivity between them was ascribed to the grain boundary conductivity. We hypothesize that the  $\text{AlPO}_4$ , which was formed by insufficient mixing of the Ti and Al sources,

would contribute to lower grain boundary conductivity by its presence near the grain boundary.

In conclusion, the Al source strongly affects the Li ion conductivity of the produced LATP. The insufficient mixing of the Ti source with the Al source causes the formation of  $\text{AlPO}_4$  impurity phase, resulting in low conductivity. Water-insoluble Al sources should be used for water-insoluble  $\text{Ti}(\text{C}_3\text{H}_7\text{O})_4$ , which is currently the most widely used Ti source.

## 5. Conclusion

The electrochemical properties of LATP that were prepared by the sol–gel method using water-soluble  $\text{Al}(\text{NO}_3)_3$  and water-insoluble  $\text{Al}(\text{C}_3\text{H}_7\text{O})_3$  as Al sources were compared. The LATP prepared from  $\text{Al}(\text{NO}_3)_3$  contained an  $\text{AlPO}_4$  impurity phase because of insufficient mixing of the water-insoluble  $\text{Ti}(\text{C}_3\text{H}_7\text{O})_4$  source with the water-soluble Al source. In contrast, in the system of water-insoluble  $\text{Ti}(\text{C}_3\text{H}_7\text{O})_4$  and  $\text{Al}(\text{C}_3\text{H}_7\text{O})_3$  sources, the formation of  $\text{AlPO}_4$  was not observed, implying that  $\text{Ti}(\text{C}_3\text{H}_7\text{O})_4$  and  $\text{Al}(\text{C}_3\text{H}_7\text{O})_3$  were mixed well in the alcohol phase. The Li ion conductivity of the LATP prepared from  $\text{Al}(\text{C}_3\text{H}_7\text{O})_3$  was higher than that from  $\text{Al}(\text{NO}_3)_3$  because the  $\text{AlPO}_4$  impurity phase would act as a resistance layer. The performance of LATP prepared by the sol–gel method is strongly affected by the Al source. Water-insoluble Al sources are suitable for water-insoluble  $\text{Ti}(\text{C}_3\text{H}_7\text{O})_4$ , which is currently the most widely used Ti source.

## References

- [1] J.M. Tarascon, M. Armand, Issues and challenges facing rechargeable lithium batteries, *Nature* 414 (2001) 359.
- [2] T. Abe, M. Ohtsuka, F. Sagane, Y. Iriyama, Z. Ogumi, Lithium ion transfer at the interface between lithium-ion-conductive solid crystalline electrolyte and polymer electrolyte, *Journal of the Electrochemical Society* 151 (2004) A1950.
- [3] H. Aono, E. Sugimoto, Y. Sadaoka, N. Imanaka, G. Adachi, Ionic conductivity of the lithium titanium phosphate ( $\text{Li}_{1+x}\text{M}_x\text{Ti}_{2-x}(\text{PO}_4)_3$ ,  $\text{M} = \text{Al}, \text{Sc}, \text{Y}$ , and  $\text{La}$ ) Systems, *Journal of the Electrochemical Society* 136 (1989) 590.
- [4] H. Aono, E. Sugimoto, Y. Sadaoka, N. Imanaka, G. Adachi, Ionic conductivity of solid electrolytes based on lithium titanium phosphate, *Journal of the Electrochemical Society* 137 (1990) 1023.
- [5] K. Takada, M. Tansho, I. Yanase, T. Inada, A. Kajiyama, M. Kouguchi, S. Kondo, M. Watanabe, Formation of  $\text{Li}_2\text{O}$  in a chemically Li-intercalated  $\text{V}_2\text{O}_5$  xerogel, *Solid State Ionics* 139 (2001) 241.
- [6] J. Fu, Superionic conductivity of glass–ceramics in the system  $\text{Li}_2\text{O} \bullet \text{Al}_2\text{O}_3 \bullet \text{TiO}_2 \bullet \text{P}_2\text{O}_5$ , *Solid State Ionics* 96 (1997) 195.
- [7] A. Hayashi, T. Konishi, K. Tadanaga, M. Tatsumisago, Formation of electrode–electrolyte interface by lithium insertion to  $\text{SnS–P}_2\text{S}_5$  negative electrode materials in all-solid-state cells, *Solid State Ionics* 177 (2006) 2737.
- [8] R. Murugan, V. Thangadurai, W. Weppner, Fast lithium ion conduction in garnet-type  $\text{Li}_7\text{La}_3\text{Zr}_2\text{O}_{12}$ , *Angewandte Chemie—International Edition* 46 (2007) 7778.
- [9] M. Kotobuki, Y. Suzuki, K. Kanamura, Y. Sato, K. Yamamoto, T. Yoshida, A novel structure of ceramics electrolyte for future lithium battery, *Journal of Power Source* 196 (2011) 9815.
- [10] M. Kotobuki, K. Kanamura, Y. Sato, K. Yamamoto, T. Yoshida, Electrochemical properties of  $\text{Li}_7\text{La}_3\text{Zr}_2\text{O}_{12}$  solid electrolyte prepared in argon atmosphere, *Journal of Power Source* 199 (2012) 346.
- [11] P. M-Manso, E.R. Losilla, M. M.-Lara, M.A.G. Aranda, S. Bruque, F.E. Mouahid, M. Zahir, High lithium ionic conductivity in the  $\text{Li}_{1+x}\text{Al}_x\text{Ge}_y\text{Ti}_{2-x-y}(\text{PO}_4)_3$  NASICON series, *Chemistry of Materials* 15 (2003) 1879.
- [12] M. Kotobuki, Y. Isshiki, H. Munakata, K. Kanamura, All-solid-state lithium battery with a three-dimensionally ordered  $\text{Li}_{1.5}\text{Al}_{0.5}\text{Ti}_{1.5}(\text{PO}_4)_3$  electrode, *Electrochimica Acta* 55 (2010) 6892.
- [13] J.S. Thokchom, B. Kumar, The effects of crystallization parameters on the ionic conductivity of a lithium aluminum germanium phosphate glass–ceramic, *Journal of Power Sources* 195 (2010) 2870.
- [14] J.K. Feng, L. Lu, M.O. Kai, Lithium storage capability of lithium ion conductor  $\text{Li}_{1.5}\text{Al}_{0.5}\text{Ge}_{1.5}(\text{PO}_4)_3$ , *Journal of Alloys Compound* 501 (2010) 255.
- [15] M. Kotobuki, K. Hoshina, Y. Isshiki, K. Kanamura, Preparation of  $\text{Li}_{1.5}\text{Al}_{0.5}\text{Ge}_{1.5}(\text{PO}_4)_3$  solid electrolyte by sol–gel method, *Phosphorus Research Bulletin* 24 (2010) 61.
- [16] K. Takada, K. Fujimoto, T. Inada, A. Kajiyama, M. Kouguchi, S. Kondo, M. Watanabe, Sol–gel preparation of  $\text{Li}^+$  ion conductive thin film, *Applied Surface Science* 189 (2002) 300.
- [17] X. Xu, Z. Wen, J. Wu, X. Yang, Preparation and electrical properties of NASICON-type structured  $\text{Li}_{1.4}\text{Al}_{0.4}\text{Ti}_{1.6}(\text{PO}_4)_3$  glass–ceramics by the citric acid-assisted sol–gel method, *Solid State Ionics* 178 (2007) 29.
- [18] M. Kotobuki, Y. Isshiki, H. Munakata, K. Kanamura, Electrochemical properties of three dimensionally ordered composite electrode between  $\text{TiO}_2$  and  $\text{Li}_{1.5}\text{Al}_{0.5}\text{Ti}_{1.5}(\text{PO}_4)_3$ , *Electrochemistry* 79 (11) (2011) 865.
- [19] J.T.S. Irvine, D.C. Sinclair, A.R. West, Electroceramics: characterization by impedance spectroscopy, *Advanced Materials* 2 (1990) 132.
- [20] V. Thangadurai, W. Weppner, Investigations on electrical conductivity and chemical compatibility between fast lithium ion conducting garnet-like  $\text{Li}_6\text{BaLa}_2\text{Ta}_2\text{O}_{12}$  and lithium battery cathodes, *Journal of Power Sources* 142 (2005) 339.
- [21] M. Kotobuki, K. Kanamura, Y. Sato, T. Yoshida, Fabrication of all-solid-state lithium battery with lithium metal anode using  $\text{Al}_2\text{O}_3$ -added  $\text{Li}_7\text{La}_3\text{Zr}_2\text{O}_{12}$  solid electrolyte, *Journal of Power Sources* 196 (2011) 7750.
- [22] J. Fu, Fast  $\text{Li}^+$  ion conduction in  $\text{Li}_2\text{O}-(\text{Al}_2\text{O}_3-\text{Ga}_2\text{O}_3)-\text{TiO}_2\text{P}_2\text{O}_5$  glass–ceramics, *Journal of Materials Science* 33 (1998) 1549.
- [23] J.L. Naraez-Semante, A.C.M. Rodrigues, Microstructure and ionic conductivity of  $\text{Li}_{1+x}\text{Al}_x\text{Ti}_{2-x}(\text{PO}_4)_3$  NASICON glass–ceramics, *Solid State Ionics* 181 (2010) 1197.